Enhancement of laser cut edge quality of ultra-thin titanium grade 2 sheets by applying in-process approach using modulated Yb:YAG continuous wave fibre laser

Moritz Burger (moritz.burger@oth-regensburg.de)
Ostbayerische Technische Hochschule Regensburg https://orcid.org/0000-0002-2221-1672
Alexander Bartsch
Marius Grad
Lukas Esper
Ulrich Schultheiß
Ulf Noster
Thomas Schratzenstaller

Research Article

Keywords: laser cutting, titanium sheet, kerf

Posted Date: February 1st, 2023

DOI: https://doi.org/10.21203/rs.3.rs-2520041/v1

Abstract

Titanium is used in many areas due to its excellent mechanical, biological and corrosion-resistant properties. Implants often have thin and filigree structures, providing an ideal application for laser fine cutting. In literature, the main focus is primarily on investigating and optimizing the parameters for titanium sheet thicknesses greater than 1 mm. Hence, in this study, the basic manufacturing parameters of laser power, cutting speed and laser pulsing of a 200 W modulated fibre laser are investigated for 0.15 mm thick titanium grade 2 sheets. A reproducible, continuous cut could be achieved using 90 W laser-power and 2 $\frac{\mathrm{mm}}{\mathrm{s}}$ cutting-speed. Pulse pause variations between 85–335 µs in 50 µs steps and fixed pulse duration of 50 µs show that a minimum kerf width of 23.4 µm, as well as a minimum cut edge roughness Rz of 3.59 µm, is achieved at the lowest pulse pause. An increase in roughness towards the laser exit side, independent of the laser pulse pause, was found and discussed. The results provide initial process parameters for cutting thin titanium sheets and thus provide the basis for further investigations, such as the influence of cutting gas pressure and composition on the cut edge.

1. Introduction

Titanium has long been used for a wide range of high-performance products. In the aerospace and marine sectors, but also in medical technology, the material has established itself due to its superior properties compared to other metallic materials.[1–4] It has a high strength-to-weight ratio, good resistance to fatigue and corrosion, and good biocompatibility.[5, 6] But compared to other established technical materials such as stainless steel, titanium is difficult to machine using conventional methods. This is due to its low modulus of elasticity ($E_{Titanium}$=105 GPa), low thermal conductivity, and strong chemical activity at elevated temperatures.[3, 4, 6] For these reasons, laser cutting is suitable as a non-contact manufacturing process for titanium.[3] The high tool wear that occurs, for example, when milling titanium can thus be avoided. In addition, laser cutting is ideal for the economical production of filigree structures due to its speed, precision, and resource efficiency.[3, 7] A variety of devices are cut with lasers from a thin base material, e.g. in the medical application for coronary stents. The requirements regarding the quality of the laser cut are high due to the filigree structures, for instance a structural width of approximately 80 µm for stents; the influence of the cut edge on the biocompatibility; and the specifications by laws and standards (EN ISO 9013:2000).[2, 8–10] To meet these requirements, it is necessary to use an inert cutting gas, such as argon. This is intended to prevent an enrichment of nitrogen and oxygen, for example, as well as the formation of microcracks in the cutting area.[2, 3, 7–9, 11]

The influence of the cutting parameters on the kerf during laser cutting of titanium has been studied in the past for sheet thicknesses greater than 1 mm.[3, 4, 7, 8, 11–15] The ideal process parameters that have been found can hardly be transferred to thinner sheet thicknesses, since, for example, the necessary laser power, cutting speed, gas pressure, etc. depend strongly and non-linearly on the material thickness to be cut.

Thus, this paper focuses on the laser fine cutting of titanium grade 2 sheets with a material thickness of 0.15 mm. The parameters investigated are laser power, cutting speed, and a suitable ratio between laser pulse and pause, as these parameters have a great influence on a reproducible and minimal kerf in thin titanium sheets.[8, 15, 16]

2. Material And Methods

The investigated sheets of titanium grade 2 have a thickness of 0.15 mm. The chemical analysis of the material is presented in Table 1, and the mechanical properties in Table 2, respectively.

Table 1
Chemical analysis of the investigated titanium grade 2 sheets

Element	**Fe**	**C**	**N**	**H**	**O**	**Ti**
Analysis wt %	0.042	0.012	0.003	0.001	0.1	Rest/Balance

Table 2
Mechanical properties of the investigated titanium grade 2 sheets

Mechanical Properties	**Value**
Tensile Strength [MPa]	433
Yield Strength [MPa]	286
Elongation [%]	33

The laser system used was a 200 W TruFiber 200P compact (Trumpf SE & Co. KG, Ditzingen, Germany) fibre laser in modulated continuous wave (cw) mode with ytterbium-doped yttrium aluminium garnet (YAG) as the active medium. The wavelength of the laser was 1068–1072 nm with a beam quality of 0.38 ± 0.03 mm*mmrad. The cutting head (Precitec GmbH & Co. KG, Gaggenau-Bad Rotenfels, Germany) has a 50 mm focal length and theoretical laser spot size of 16 µm, as well as an internal cutting gas supply to the Ø 0.2 mm cutting nozzle. The focus position of the laser was adjusted to the middle of the sheet thickness. All tests were carried out with 10 bar argon 5.0 cutting gas pressure - measured at the cutting nozzle. The cutting gas pressure corresponded to a flow rate of 30 $\frac{l}{min}$. The cutting table used was an ATS100 two axis traverse table (Aerotech GmbH, Fürth, Germany) with a repeatability of ± 0.3 µm and accuracy of ± 9 µm. The laser scanning microscope measurements were performed with an Olympus Lext 3D Measuring Laser Microscope OLS400 (Olympus Europa SE & Co. KG, Hamburg, Germany) with a laser wavelength of 400–420 nm. The cut-off distance λ_c for the roughness measurements was 80 µm.

In Fig. 1, the laser cutting process with an internal cutting gas supply is shown schematically. It is visible how the molten material is ejected downwards through the cutting gas flow. The resulting kerf with its characteristic shape and area of influence known as the heat-affected zone (HAZ), is shown in Fig. 2.

In the first step of the investigation, a process window is to be found in which a square cutting pattern (see Fig. 3) can be reliably and continuously cut and detached from the sheet without mechanical effort.

The cutting speed is varied (2–10 $\frac{\mathrm{mm}}{\mathrm{s}}$) for each selected laser power level (50–120 W in 10 W steps). Subsequently, the cut samples were placed in an ultrasonic bath, Sonorex Super RK 102H (BANDELIN electronic GmbH & Co. KG, Berlin, Germany); in 350 ml deionised water; and 30 ml ethanol for 5 minutes. The samples remained freely immersed in the medium and had no wall contact in the ultrasonic bath.

A cut is considered complete and successful when the cut square has detached independently from the sheet metal. With the identified parameters of power and cutting speed, a process window for a reproducible, continuous laser cut could be found.

Secondly, the influence of the laser pause on the width and roughness of the kerf was investigated. For this purpose, the sample geometry shown in Fig. 4 was cut with the previously determined power and speed at different pulse pauses (85–335 µs in 50 µs steps) and a fixed pulse duration of 50 µs. Each sample contains five open and five closed kerfs. For the open kerf gaps, kerf gap roughness (Ra, Rz) and for the closed kerf gaps, kerf gap width were investigated using CLSM. The roughness measurements were taken along the kerf in 4 different planes parallel to the sheet surface. The first measurement was taken 8 µm below the sheet surface as seen from the laser entry side. The other measurements were taken at an incremental distance of 40 µm below. (measurement positions schematically shown in Figure 4). Figure 5 shows an exemplary laser cycle with pulse duration and pause.

3. Results And Discussion

3.1. Variation of laser power and cutting speed

The combination of laser power and cutting speed was varied from 50–120 W and 2–10 $\frac{\mathrm{mm}}{\mathrm{s}}$, respectively. The quadratic cut patterns were treated with ultrasonic bath and it was determined whether the squares could be detached by this treatment. This serves as proof that the kerf is sufficiently large and continuous. Unsuitable cutting parameters lead to wedging of the opposite sides of the ultra-thin titanium sheet, which makes it difficult to detach the cut squares, as shown in Fig. 6.

Figure 7 shows, as the laser power increases, the probability of detachment increases. As the cutting speed increases, the probability of detachment increases also. At a laser power of at least 90 W, all squares detached, regardless of the cutting speed. This power was assessed as sufficient and used for the further investigations. In this case the lower the cutting speed, the more heat is introduced into the cutting geometry.

Also, this additional heat input could lead to an unintended change in the microstructure.[3, 17] In addition, at a higher cutting speed, less time is required for a given cut length, which is highly important in terms of economic aspects. The most suitable parameters for the following results are a laser power of 90 W and a cutting speed of 10 $\frac{\mathrm{mm}}{\mathrm{s}}$.

3.2. Variation of the pulse pause

Figure 8 shows the influence of the pulse pause at a fixed pulse duration (50 µs) on the width of the kerf. The theoretical minimum laser spot size of the laser system of 16 µm is also shown. The kerf width increases with increasing pulse pause. The minimum kerf width of 23.4 µm is reached at the lowest investigated pulse pause of 85 µs. This corresponds to a deviation from the theoretical spot size by almost 46%.

When the energy of the laser is coupled into the material, areas that were not directly exposed are heated and liquefied also, which is why the actual kerf is always larger than the theoretical laser spot size. The liquefied material is transported out of the kerf by the cutting gas flow. The smaller the pulse break, the greater the average thermal energy affecting the cutting geometry. As a result, the molten material heats up to higher temperatures in this area. Due to the resulting decrease in viscosity, the material is more effectively conveyed out of the kerf by the cutting gas flow. An increased viscosity, which is obtained when using a larger pulse gap, allows the thermal energy of the molten material to be partially transferred to the adjacent area, which in turn also leads to a melting of this area. These two effects influence each other, but each leads to an increase in the kerf width. The maximum kerf width of 30.2 µm, as displayed in Fig. 8, was achieved with a pulse pause of 285 µs. The displayed roughness values in Fig. 9 are the average of four measurements at different profile depths which are schematically shown in Fig. 4. It can be observed that at the shortest pulse pause duration of 85 µs, a minimum roughness Rz of 4.98 µm and Ra of 0.81 µm could be achieved.

Figure 10 shows that the cutting edge roughness increases from the laser entrance to the laser exit side, independent of the pulse pause duration. The line roughness (Ra and Rz) was measured along the kerf. Figure 10: Cutting edge roughness measured from laser entry to laser exit side Noticeably, for pulse durations of 85 µs and 135 µs, the lowest roughness Rz of 3.59 µm and 3.44 µm was measured at a distance of 8 µm from the top of the sheet. For longer pulse pauses, higher roughness of Rz > 4.50 µm are observed at the similar location.

The measured Rz values increase for all pulse pause durations with increasing measurement depth from the laser entrance side. This correlation can be observed in Fig. 11, where the presence of slag and molten material is shown using 185 µs pulse pause as an example. With pulse durations of 135 µs or shorter, the pause between two pulses is just small enough to ensure that the coupled power density and the associated temperature increase are sufficient to constantly liquefy the material near the surface. This state of aggregation promotes expulsion of molten material and thus lowers the surface roughness. At higher pulse pauses, as well as in areas of the titanium sheet far from the surface, the coupled power density and the resulting temperature increase of the material are not sufficient to ensure constant

liquefaction. On the edge of the cut, splatters can be seen against the direction of the cut. The formation of these can be explained in two ways. A partially-liquefied melted material offers such great resistance to the argon flow that it is dispersed when it is expelled, or else a liquid melted material meets a solid resistance and is dispersed by it. This can explain the increased surface roughness and the structural formations in Fig. 11.

4. Conclusion

For industrial laser cutting of small structures, a minimum cutting gap is necessary. To achieve this, the following findings were obtained in this work:

- With a laser power of 90 W and a cutting speed of 10 $\frac{\mathrm{mm}}{\mathrm{s}}$, reproducible, continuous cuts of square shapes in 0.15 mm thick titanium grade 2 sheets could be achieved
- The minimum cutting gap of 23.4 µm was achieved with a pulse pause of 85 µs and pulse duration of 50 µs
- The kerf width increases with higher pulse pauses
- The minimum cutting edge roughness of 4.98 µm was achieved with a pulse pause duration of 85 µs

It should also be noted that the resulting burr at the cut edges still requires post-processing, depending on the quality requirements of the end product. Even at lower laser powers, which were identified as insufficient in this article, ultra-thin titanium sheets could be cut with a suitable post-treatment strategy. This post-processing should be taken into consideration when optimizing the cutting edges, and should be the focus of further work.

Declarations

Author contribution

Alexander Bartsch: concept, sample preparation, data processing, writing, editing

Prof. Dr.-Ing. Thomas Schratzenstaller: concept, editing, proofreading

Moritz Burger: concept, sample preparation, data processing, writing, editing

Marius Grad: writing, editing, sample analysis (LSM)

Lukas Esper: sample preparation, data processing, editing, graphics

Ulrich Schultheiß: sample preparation, SEM analysis, editing

Prof. Dr.-Ing. Ulf Noster: editing, article preparation, proofreading

Aknowledgement

The authors acknowledge the support of Jan Zentgraf and Philipp Lulla (Medical Device Lab, OTH Regensburg, Regensburg, Germany) for their insight and feedback on this publication, as well as Anna Koffler (Medical Device Lab, OTH Regensburg, Regensburg, Germany) for her help with laser-scanning and light microscopy imaging.
Research grant/project "*OrbitaTreat"* by the Bayerische Forschungsstiftung (BFS); Funding Nr. AZ-1369-19. Regensburg Center of Health Sciences and Technology (RCHST) and Regensburg Center of Biomedical Engineering (RCBE)

Disclosure statement

The authors report there are no competing interests to declare

References

1. Thakre PR, Singh RP, Slipher G. Mechanics of Composite, Hybrid and Multifunctional Materials, Volume 5. Cham: Springer International Publishing; 2019.
2. Mukherjee S, Dhara S, Saha P. Laser surface remelting of Ti and its alloys for improving surface biocompatibility of orthopaedic implants. Materials Technology 2018;33(2):106–18. https://doi.org/10.1080/10667857.2017.1390931.
3. Scintilla LD, Sorgente D, Tricarico L. Experimental Investigation on Fiber Laser Cutting of Ti6Al4V Thin Sheet. AMR 2011;264-265:1281–6. https://doi.org/10.4028/www.scientific.net/AMR.264-265.1281.
4. Shrivastava PK, Pandey AK. Multi-Objective Optimization of Cutting Parameters during Laser Cutting of Titanium Alloy Sheet using Hybrid approach of Genetic Algorithm and Multiple Regression Analysis. Materials Today: Proceedings 2018;5(11):24710–9. https://doi.org/10.1016/j.matpr.2018.10.269.
5. Kaur M, Singh K. Review on titanium and titanium based alloys as biomaterials for orthopaedic applications. Mater Sci Eng C Mater Biol Appl 2019;102:844–62. https://doi.org/10.1016/j.msec.2019.04.064.
6. Niinomi M, Liu Y, Nakai M, Liu H, Li H. Biomedical titanium alloys with Young's moduli close to that of cortical bone. Regen Biomater 2016;3(3):173–85. https://doi.org/10.1093/rb/rbw016.
7. Yilbas BS, Shaukat MM, Ashraf F. Laser cutting of various materials: Kerf width size analysis and life cycle assessment of cutting process. Optics & Laser Technology 2017;93:67–73. https://doi.org/10.1016/j.optlastec.2017.02.014.
8. Pandey AK, Dubey AK. Modeling and optimization of kerf taper and surface roughness in laser cutting of titanium alloy sheet. J Mech Sci Technol 2013;27(7):2115–24. https://doi.org/10.1007/s12206-013-0527-7.
9. Rao BT, Kaul R, Tiwari P, Nath AK. Inert gas cutting of titanium sheet with pulsed mode CO2 laser. Optics and Lasers in Engineering 2005;43(12):1330–48.

https://doi.org/10.1016/j.optlaseng.2004.12.009.

10. Wiesent L, Schultheiß U, Schmid C, Schratzenstaller T, Nonn A. Experimentally validated simulation of coronary stents considering different dogboning ratios and asymmetric stent positioning. PLoS One 2019;14(10):e0224026. https://doi.org/10.1371/journal.pone.0224026.
11. Pramanik D, Kuar AS, Sarkar S, Mitra S. Enhancement of sawing strategy of multiple surface quality characteristics in low power fiber laser micro cutting process on titanium alloy sheet. Optics & Laser Technology 2020;122:105847. https://doi.org/10.1016/j.optlastec.2019.105847.
12. Kochergin SA, Morgunov Y, Saushkin BP. Particularities of Pulse Laser Cutting of Thin Plate Titanium Blanks. Procedia Engineering 2017;206:1161–6. https://doi.org/10.1016/j.proeng.2017.10.611.
13. Boujelbene M, El Aoud B, Bayraktar E, Elbadawi I, Chaudhry I, Khaliq A et al. Effect of cutting conditions on surface roughness of machined parts in CO2 laser cutting of pure titanium. Materials Today: Proceedings 2021;44:2080–6. https://doi.org/10.1016/j.matpr.2020.12.179.
14. Muzammil M, Chandra A, Kankar PK, Kumar H. Recent Advances in Mechanical Engineering. Singapore: Springer Singapore; 2021.
15. Anghel C, Gupta K, Mashamba A, Jen T-C. Recent Developments in Laser Cutting of Metallic Materials. In: Proceedings of the International Conference on Industrial Engineering and Operations Management, p. 1881–1891.
16. Saptaji K, Gebremariam MA, Azhari MABM. Machining of biocompatible materials: a review. Int J Adv Manuf Technol 2018;97(5-8):2255–92. https://doi.org/10.1007/s00170-018-1973-2.
17. Shanjin L, Yang W. An investigation of pulsed laser cutting of titanium alloy sheet. Optics and Lasers in Engineering 2006;44(10):1067–77. https://doi.org/10.1016/j.optlaseng.2005.09.003.

Figures

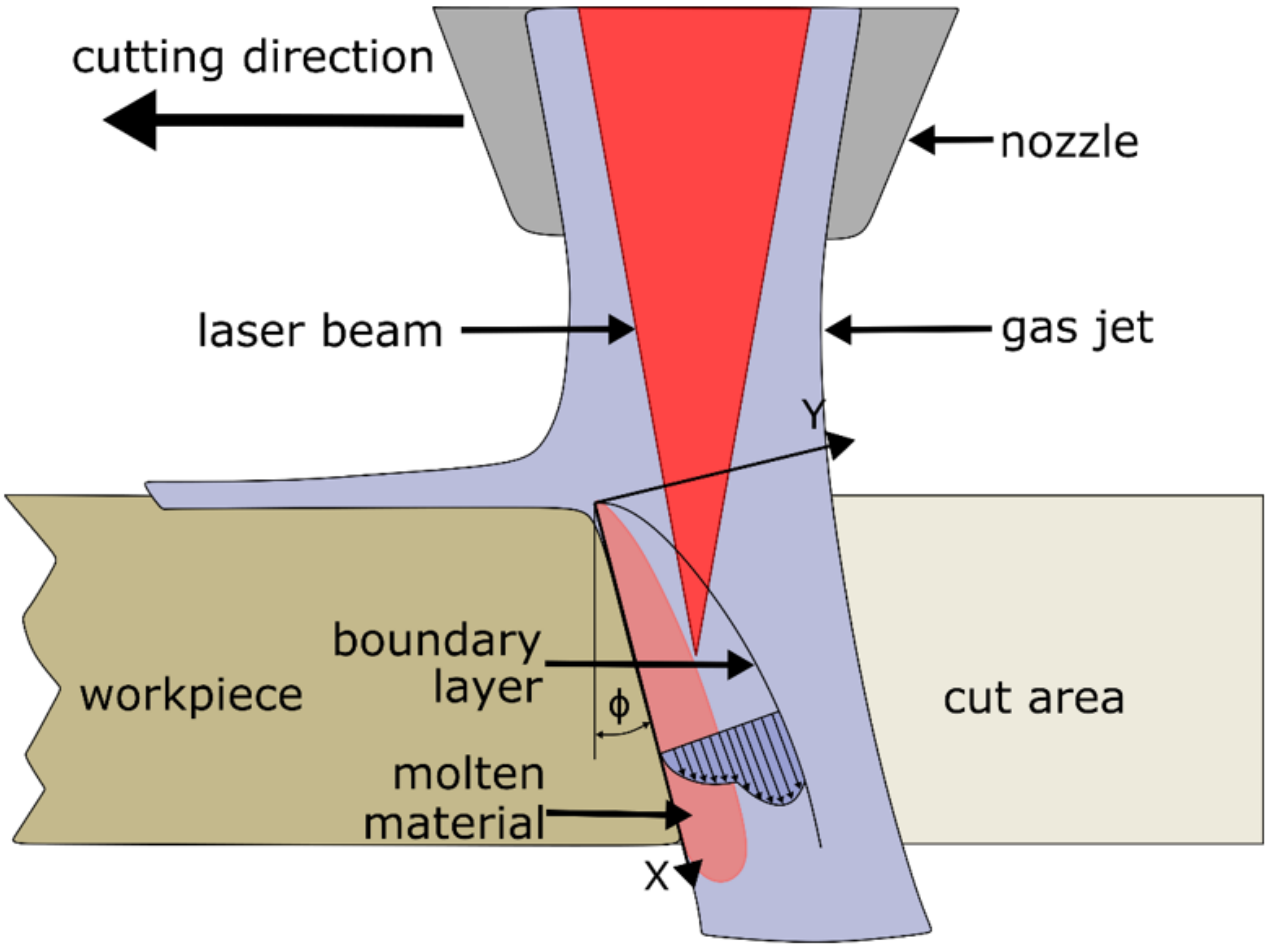

Figure 1

Schematic laser cutting process with an internal cutting gas supply (modified according to [1])

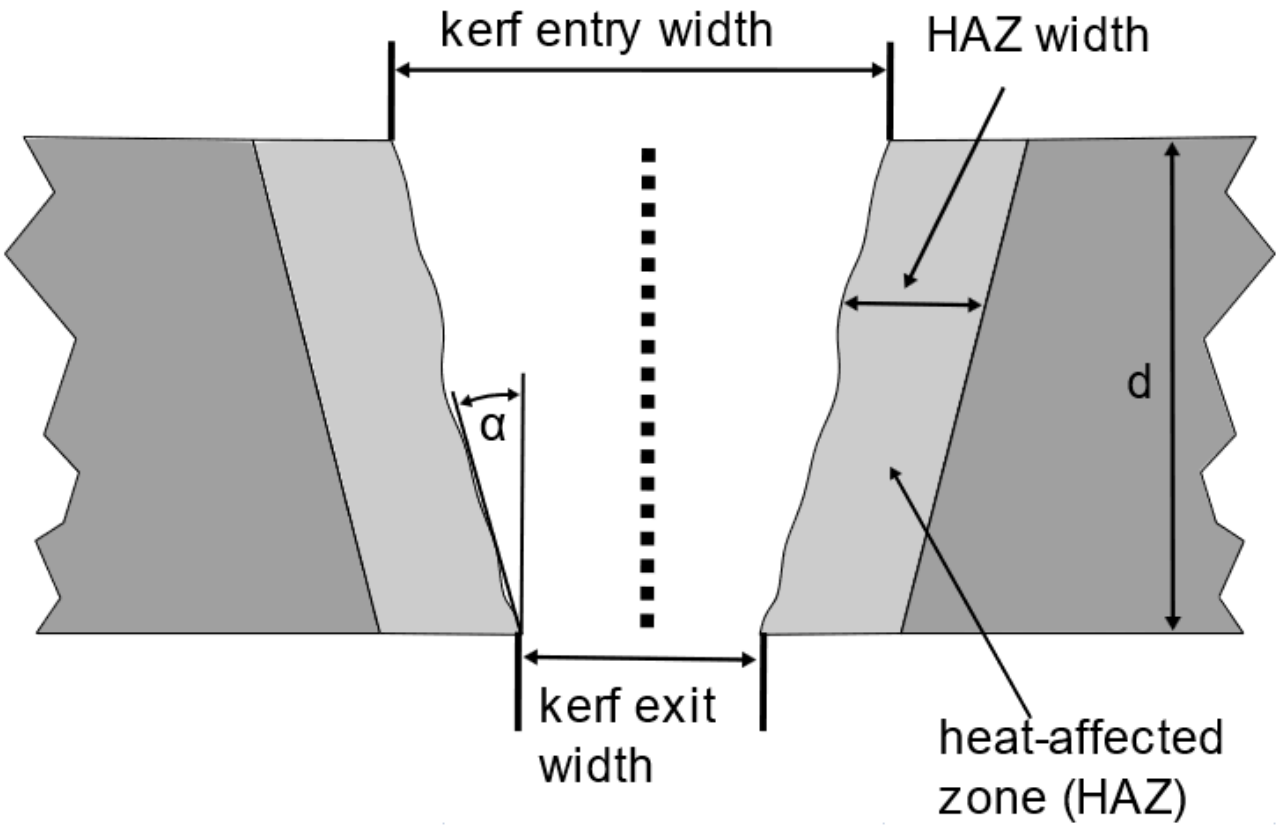

Figure 2

Resulting characteristic kerf after laser cutting

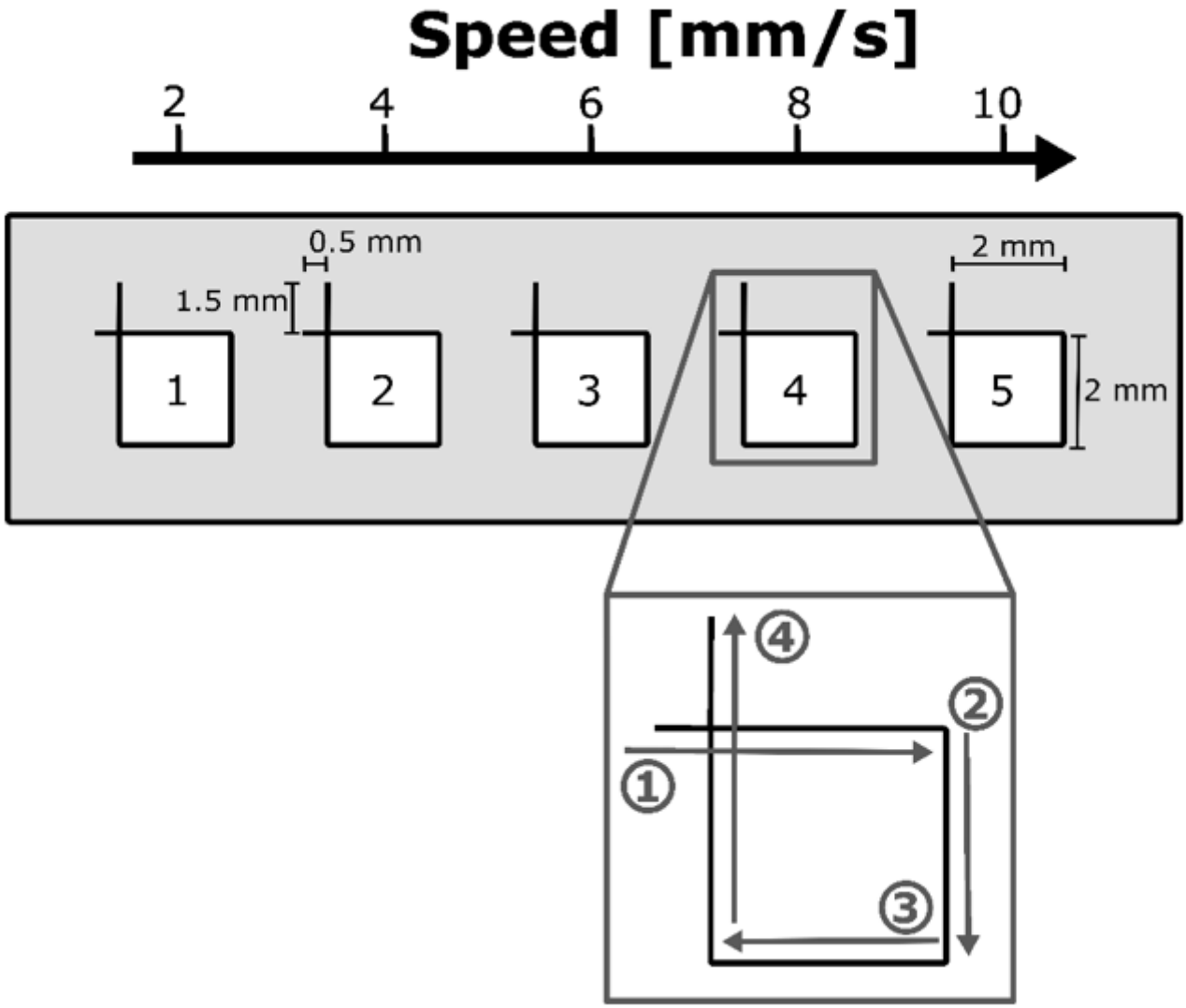

Figure 3

Quadratic cutting pattern with applied cutting sequence of the laser at a constant power level and variation of the cutting speed; entry and exit lanes of the laser are shown for the acceleration of the two axis traverse table, as well as the laser switch-on delay

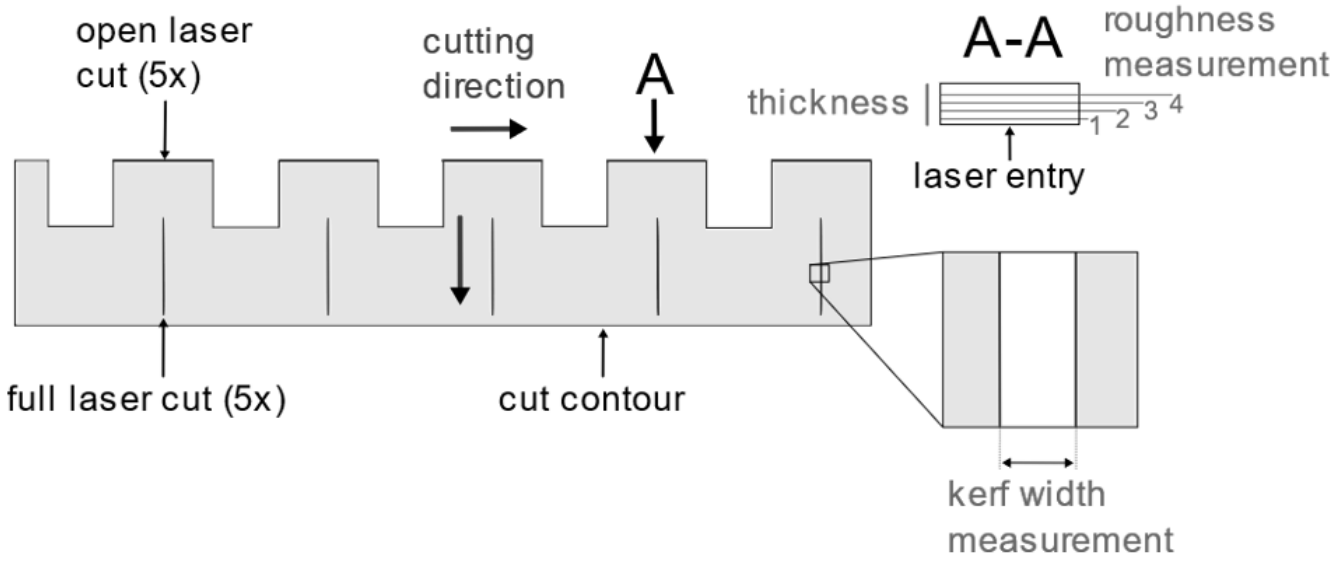

Figure 4

Sample geometry for the investigation of laser pulsing on kerf width and roughness

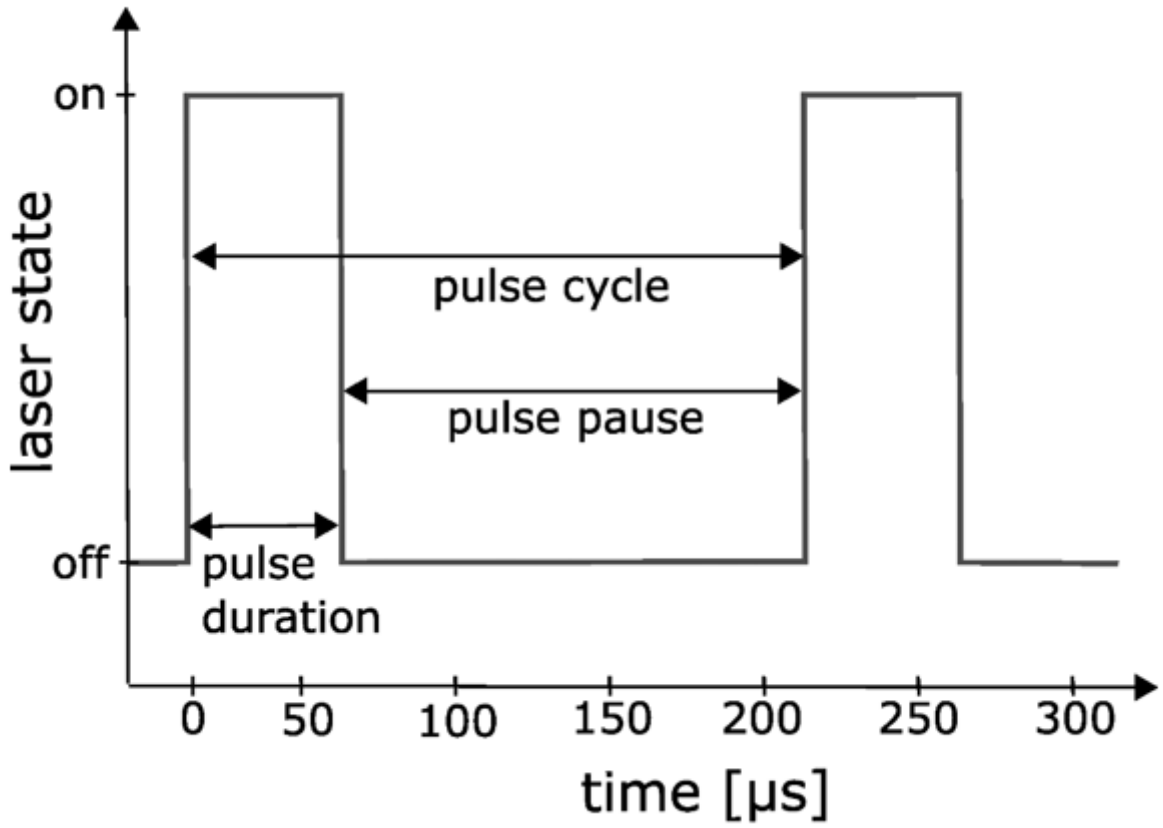

Figure 5

Schematic laser cycle with laser pulse, pause, and cycle time

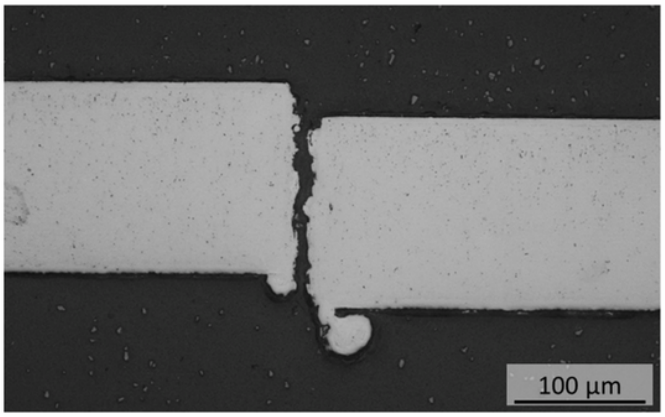

Figure 6: Non-detached laser-cut square (on the right side) at a laser power of 70 W and 10 $\frac{\text{mm}}{\text{s}}$

Figure 6

See image above for figure legend

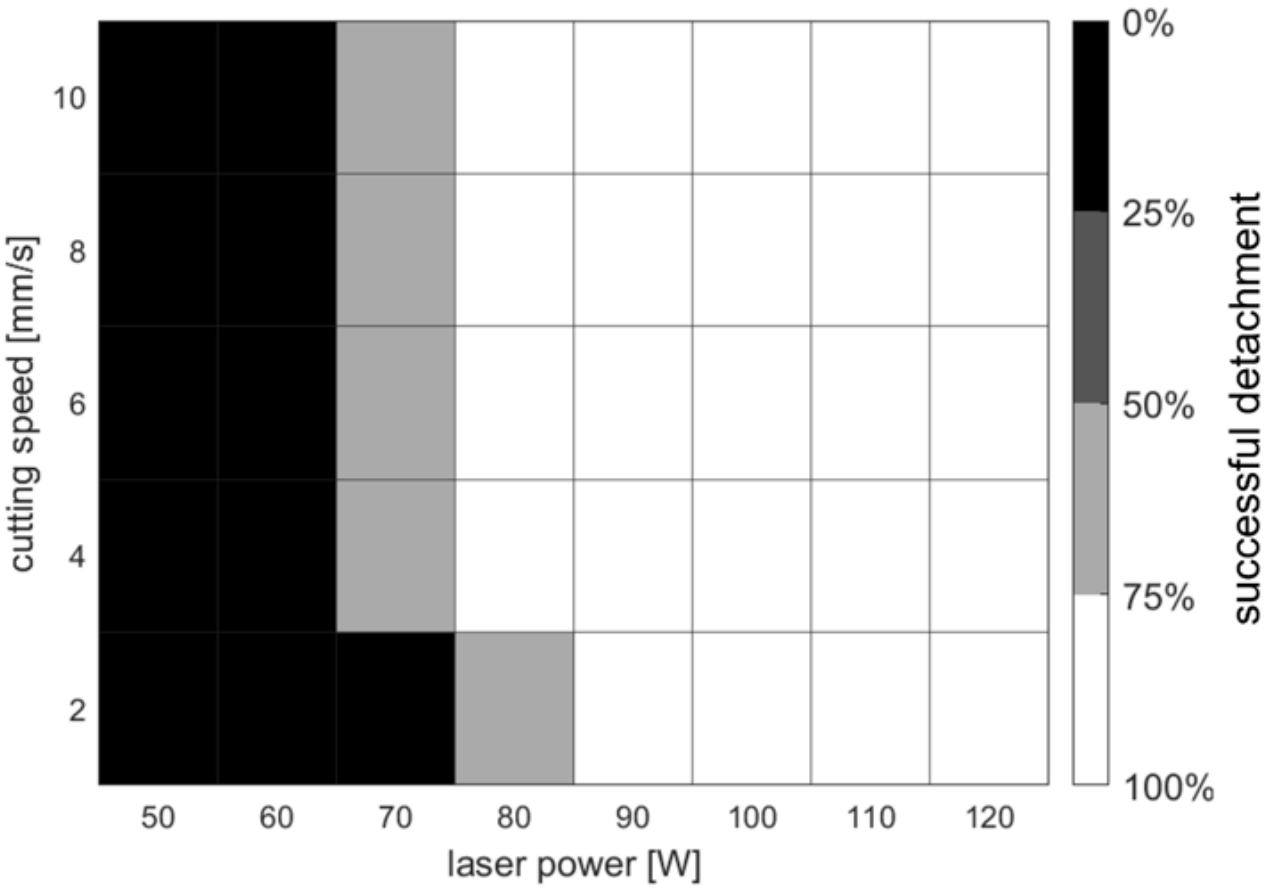

Figure 7

Successful detachment in ultrasonic bath of cut squares as a criterion for a valid laser cut

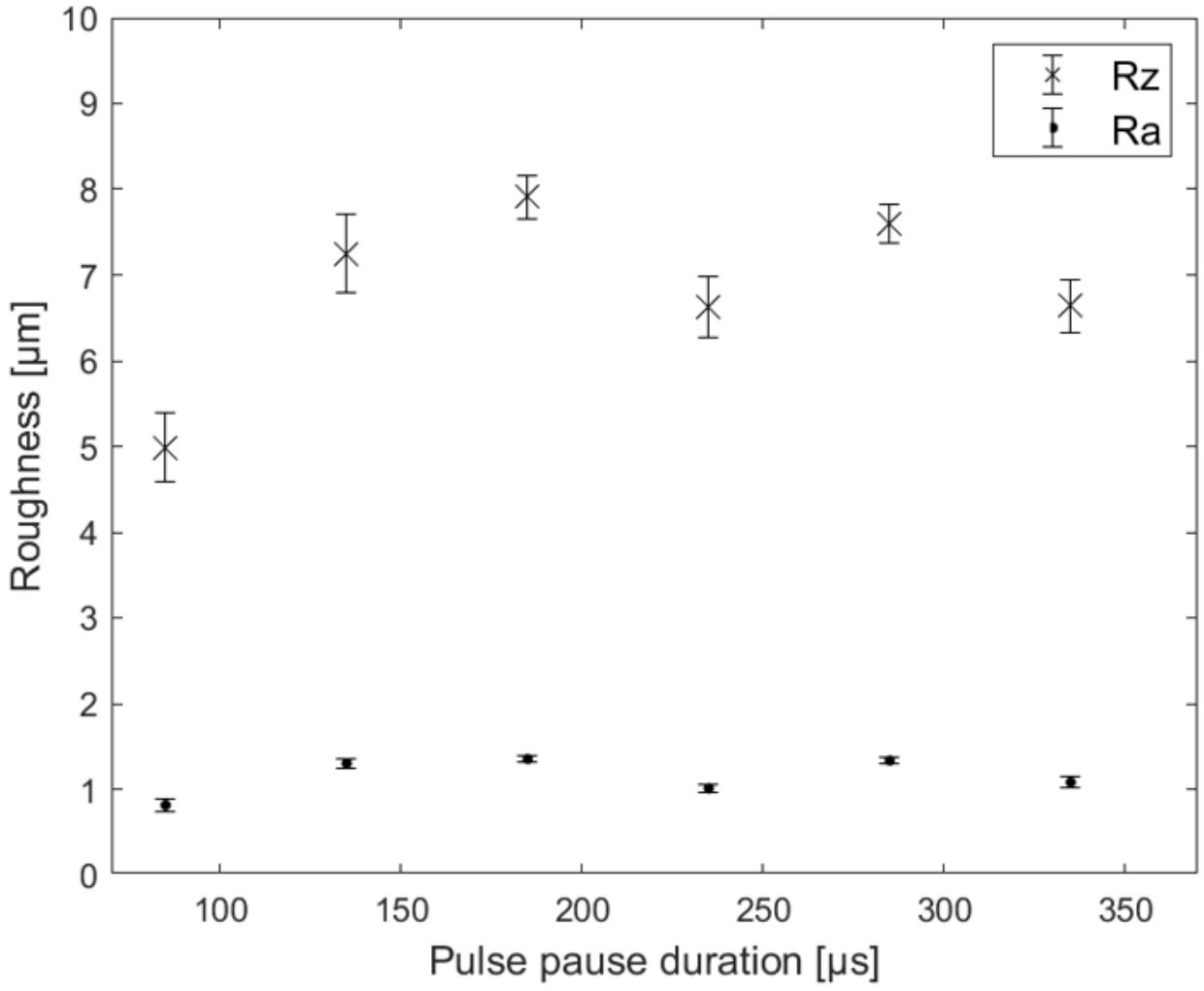

Figure 8

Influence of the laser pulse pause on kerf width; the theoretical laser spot size of the laser system used is 16 µm

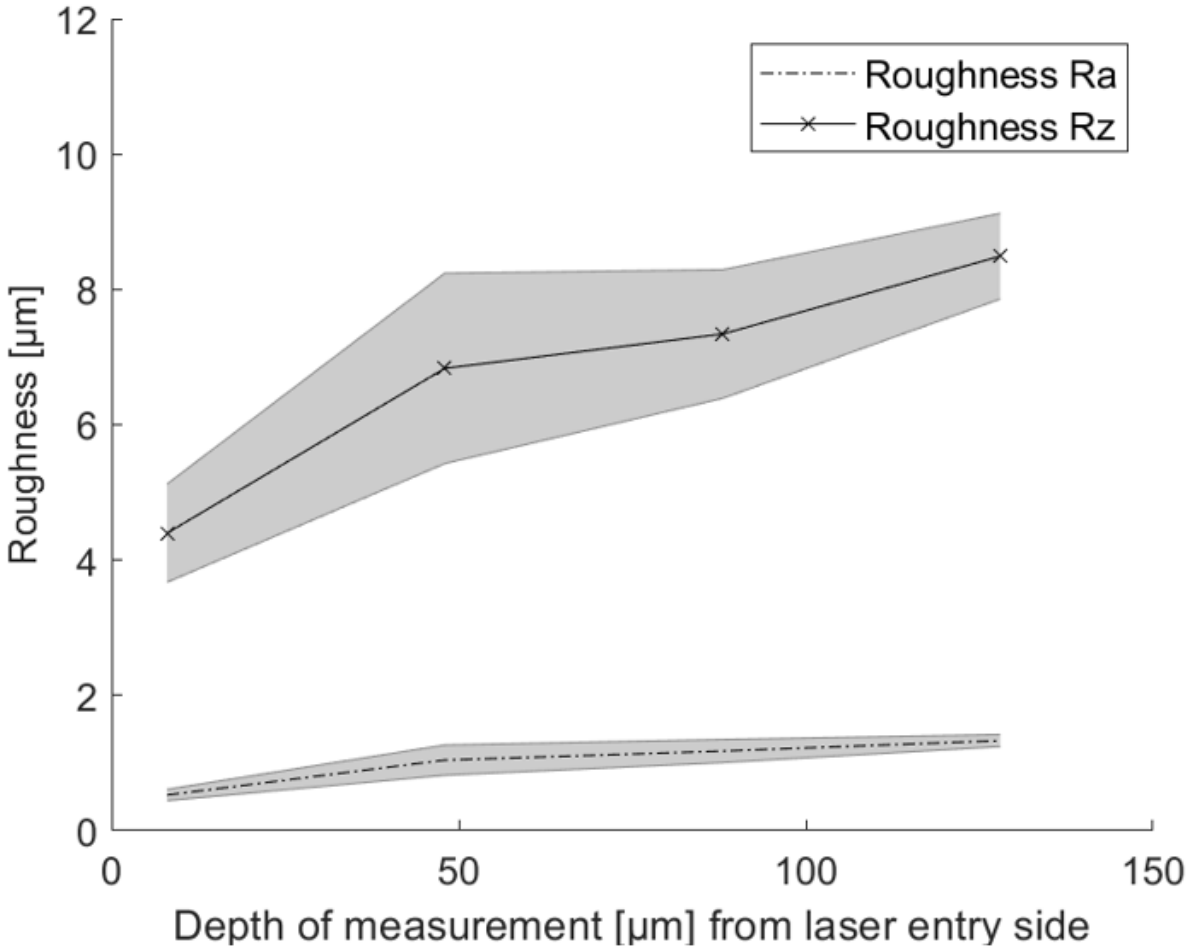

Figure 9

Cutting edge roughness for different pulse pause durations

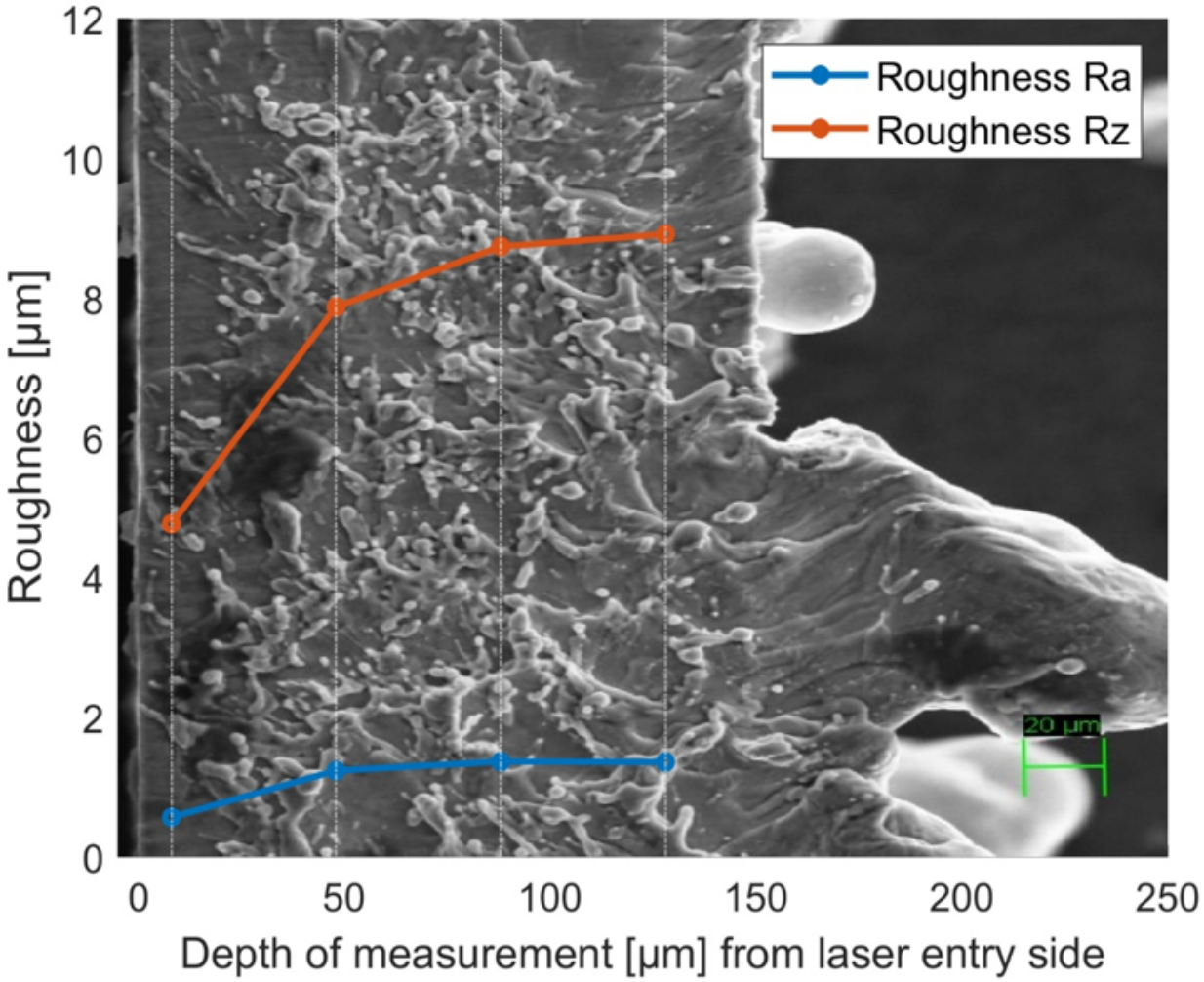

Figure 10

Cutting edge roughness measured from laser entry to laser exit side